

Electrical resistivity and thermopower of single-crystal $R\text{Ni}_2\text{B}_2\text{C}$ ($R=\text{Dy, Ho, Er, Tm}$) magnetic superconductors

A. K. Bhatnagar

*Physics Department, Texas A&M University, College Station, Texas 77843-4242
and Physics Department, University of Hyderabad, Hyderabad 500046, India*

K. D. D. Rathnayaka and D. G. Naugle

Physics Department, Texas A&M University, College Station, Texas 77843-4242

P. C. Canfield

Physics Department, Ames Laboratory and Iowa State University, Ames, Iowa 50011

(Received 8 January 1997)

The in-plane resistivity ρ and thermopower S of single crystal $R\text{Ni}_2\text{B}_2\text{C}$ ($R=\text{Dy, Ho, Er, Tm}$) has been measured from 4 to 300 K. The resistivity is linear in temperature from about 100 to 300 K, but the low-temperature dependence goes as T^p with $p=3.0, 2.6, 2.0,$ and $1.4,$ respectively, from Dy to Tm, in comparison to the T^2 behavior previously reported for $\text{LuNi}_2\text{B}_2\text{C}$. The thermopower exhibits a region linear in T from about 100 to 300 K where the coefficient b scales by the de Gennes factor $(g-1)^2J(J+1)$ for different $R=\text{Lu, Tm-Dy}$. The quantity $S-bT$ is surprisingly similar in temperature dependence and magnitude for samples with $R=\text{Y, Lu, Dy-Tm}$, suggesting a common, nonmagnetic contribution to the thermopower of these compounds. [S0163-1829(97)07625-X]

I. INTRODUCTION

The recently discovered quaternary borocarbide intermetallic compounds $R\text{Ni}_2\text{B}_2\text{C}$, where R is Y or a rare-earth element (Lu-Gd), exhibit a wide variety of physical properties. The structure of these compounds is body-centered tetragonal (space group $I4/mmm$) with alternating square planar layers of rare-earth carbides and corrugated Ni_2B_2 sheets with a unit cell consisting of two formula units,¹ a layered structure similar to that of ThCr_2Si_2 with an additional carbon atom per rare-earth atom in the rare-earth layer and reminiscent of the layered high- T_c cuprates. Their physical properties depend upon the R atom; compounds with $R=\text{Y, Lu}$ seem to be BCS-type superconductors² with relatively high T_c [$T_c(\text{Y})=15.6$ K, $T_c(\text{Lu})=16.1$ K]; $R=\text{Dy, Ho, Er, and Tm}$ exhibit the coexistence of superconductivity and magnetic order (generally antiferromagnetic), as observed earlier in the magnetic superconductors $RRh_4\text{B}_4$ and $R\text{Mo}_6\text{S}_8$,³ with additional effects due to anisotropy induced by crystalline electric fields;⁴⁻⁸ $R=\text{Tb}$ (Ref. 9) and Gd (Ref. 10) do not show superconductivity at least above 0.5 and 1.4 K, respectively; $R=\text{Yb}$ displays heavy-fermion behavior and is not superconducting down to 0.34 K.¹¹ The borocarbides, which show superconductivity, are type-II superconductors with a small coherence length ($\approx 50-100$ Å). Electronic band structure calculations on $\text{LuNi}_2\text{B}_2\text{C}$ (Refs. 12 and 13) and $\text{YNi}_2\text{B}_2\text{C}$ (Ref. 14) show that the states near the Fermi level E_F are dominated mainly by the Ni(3d) character and have a relatively high density of states at E_F . The bridging carbon atoms provide strong interlayer interactions, resulting in the three-dimensional nature of the compounds.¹⁵ The superconductivity is believed to originate in the Ni_2B_2 layers. Theoretical studies¹²⁻¹⁴ as well as some experimental

reports¹⁶⁻²¹ indicate that these are moderately strong-coupling superconductors. Many experimental results indicate that these compounds are the conventional phonon-mediated s -wave superconductors, although some deviations are reported, namely, the absence of the coherent peak in the NMR relaxation rate below T_c ,²² T^3 dependence of the specific heat in a wide range of temperatures below T_c ,¹⁶ and an anomalous temperature dependence of H_{c1} , $\lambda(T, H=0)$, and microwave impedance.²³

The compounds $R\text{Ni}_2\text{B}_2\text{C}$ with $R=\text{Ho, Dy, Er, and Tm}$, which exhibit coexistence of superconductivity and magnetic order, have been the subject of intense research. $\text{HoNi}_2\text{B}_2\text{C}$, $\text{ErNi}_2\text{B}_2\text{C}$, and $\text{TmNi}_2\text{B}_2\text{C}$ have superconducting transition temperatures 8.5, 10.5, and 11 K and Néel temperatures (T_N) $\approx 5, \approx 6,$ and ≈ 1.5 K, respectively. Thus, in these three compounds, $T_N < T_c$. In contrast, $\text{DyNi}_2\text{B}_2\text{C}$ has $T_c \approx 6.2$ K and $T_N \approx 10.4$ K, i.e., $T_N > T_c$. Specific heat and magnetic susceptibility measurements on $\text{HoNi}_2\text{B}_2\text{C}$ indicate the presence of three magnetic phase transitions at 6.0, 5.5, and 5.2 K in zero magnetic field.²⁴ Neutron studies on this compound indicate that initially a long-wavelength spiral magnetic structure develops at 6 K,²⁵ which produces a deep minimum in the critical field as the ordered moment increases.⁵ Near 5 K (and zero field), a transition to a commensurate antiferromagnetic structure takes place, resulting in ferromagnetic holmium-carbide sheets with alternating directions of the magnetization, which leads to a sharp increase in the critical field with the coexistence of antiferromagnetic order down to the lowest temperature. The transition at ≈ 5.5 K, although visible in measurements of specific heat and magnetic susceptibility, has not been confirmed by the neutron studies. For $\text{ErNi}_2\text{B}_2\text{C}$, a similar sharp minimum in the critical field is observed in the vicinity of the magnetic

ordering temperature. Neutron-diffraction studies on $\text{DyNi}_2\text{B}_2\text{C}$ show that the compound is a simple collinear antiferromagnet below 10 K; the moments are aligned ferromagnetically in each rare-earth carbon layer perpendicular to the c axis with the magnetic moments of two consecutive layers aligned in opposite directions.²⁶ Neutron studies on $\text{ErNi}_2\text{B}_2\text{C}$ show that the antiferromagnetic structure developed at $T_N=6.0$ K is always incommensurate and does not display ferromagnetic basal-plane sheets of Er atoms.²⁷ Neutron-scattering results have not been reported for the Tm compound, but magnetic measurements indicate that the easy axis is along the c axis. Thus these four compounds exhibit interesting magnetic structure features which influence their superconducting behavior, although their crystallographic structure is similar.

It is important to understand the normal-state transport properties of superconductors in order to investigate possible interactions which may be responsible for the superconductivity. Recently, good single crystals of most of the borocarbide compounds have become available which provide a unique opportunity to investigate the normal-state transport properties of well-characterized samples without the granularity problems present in polycrystalline samples, which could be detrimental to the interpretation of the results on transport properties. In this paper we present the results of *detailed* studies on in-plane electrical resistivity and thermopower in single crystals of $R\text{Ni}_2\text{B}_2\text{C}$, where $R=\text{Dy}$, Ho, Er, and Tm. Brief Reports on normal-state transport properties of $R\text{Ni}_2\text{B}_2\text{C}$ have been recently presented^{28,29} by our group along with a detailed study of the transport in nonmagnetic superconductors³⁰ with $R=\text{Y}$, Lu. Recently, a brief report on the thermopower measurements of polycrystalline $\text{Y/LuNi}_2\text{B}_2\text{C}$ has also been published.³¹

II. EXPERIMENT

Single crystals of $\text{DyNi}_2\text{B}_2\text{C}$, $\text{HoNi}_2\text{B}_2\text{C}$, $\text{ErNi}_2\text{B}_2\text{C}$, and $\text{TmNi}_2\text{B}_2\text{C}$ were grown by a Ni_2B flux method.³² As-grown crystals are platelike with mostly irregular surfaces in the ab plane and usually weigh about a few hundred milligrams. Surfaces of the crystals are shiny and exhibit metallic luster, but have some roughness. Samples for electrical resistance and thermopower measurements are taken from the same single-crystal ingot (or same batch) and are prepared in a parallelepiped shape having typical dimensions of $1.5\text{ mm}\times 0.5\text{ mm}\times 0.1\text{ mm}$ after polishing the surfaces to remove the surface roughness and to make them uniformly thick. Both electrical resistance and thermopower are measured from room temperature ($\approx 295\text{ K}$) down to 4.2 K in separate low-temperature cryostats described earlier.^{5,30} The accuracy of the measurements in resistivity is better than 5% and that for the thermopower is $\pm 0.1\text{ }\mu\text{V/K}$.

III. RESULTS AND DISCUSSION

A. Resistivity

Figure 1 shows the temperature dependence of the in-plane resistivity ρ_{ab} of single crystals of $\text{DyNi}_2\text{B}_2\text{C}$, $\text{HoNi}_2\text{B}_2\text{C}$, $\text{ErNi}_2\text{B}_2\text{C}$, and $\text{TmNi}_2\text{B}_2\text{C}$ from room temperature (RT) down to 4.2 K in zero applied magnetic field. Room-temperature (RT= 295 K) resistivities are listed in

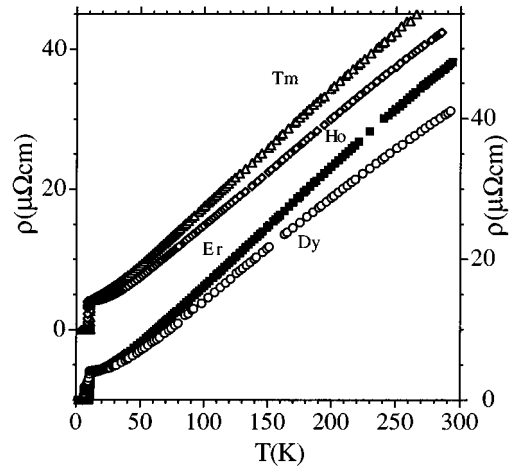


FIG. 1. Resistivity of $\text{DyNi}_2\text{B}_2\text{C}$ (circles), $\text{ErNi}_2\text{B}_2\text{C}$ (squares), $\text{HoNi}_2\text{B}_2\text{C}$ (diamonds), and $\text{TmNi}_2\text{B}_2\text{C}$ (triangles) single crystals as a function of temperature.

Table I for the Dy, Ho, Er, and Tm samples along with the value for Lu for comparison. The value of $\rho_{ab}(\text{RT})$ for $\text{DyNi}_2\text{B}_2\text{C}$ in this work is about 25% smaller than the value reported by Cho *et al.*¹⁷ although $\rho_{ab}(\text{RT})$ of $\text{ErNi}_2\text{B}_2\text{C}$ is similar to theirs within experimental error. This difference in the $\rho_{ab}(\text{RT})$ values in single crystals of these materials may arise from the slightly different growth conditions of the single crystals from batch to batch. The reported room-temperature values of the resistivity of polycrystalline $R\text{Ni}_2\text{B}_2\text{C}$ ($R=\text{Dy}$, Ho, Er, Tm) in the literature are usually much higher and have a large spread due to varying preparation conditions, weak links between the grains, and the nature of the intergranular contact material.

The temperature dependence of ρ_{ab} (to be referred as ρ hereafter) is linear from RT down to $\approx 100\text{ K}$ for the four samples, although a very small negative curvature is present near room temperature since a least-squares fit (LSF) of ρ vs T data to an expression $\rho=A'+BT+CT^2$ improves the fit as determined from the correlation coefficient. The coefficient C is negative and very small, approximately four orders of magnitude smaller than the coefficient B , and hence $\rho \propto T$ is considered to be a valid assumption for further analysis. The values of $[d\rho/dT]_{\text{RT}}$ are given in the Table I for the Dy, Ho, Er, and Tm samples and are similar to those reported for $\text{Y/LuNi}_2\text{B}_2\text{C}$ single crystals.²⁸⁻³⁰ The departure from the linear temperature dependence of the resistivity becomes significant below 50 K . Figure 2 shows ρ vs T data for $\text{DyNi}_2\text{B}_2\text{C}$ for $T < 12\text{ K}$. The resistivity for the Dy sample shows a sudden decrease in resistivity at $T=10.5\text{ K}$, which is identified as the Néel temperature (T_N) at which antiferromagnetic ordering takes place in the sample, and agrees with similar observations by others in the $\text{DyNi}_2\text{B}_2\text{C}$ polycrystalline and single-crystal samples.^{7,33} The decrease in the resistivity at the Néel temperature is caused by the decrease in the electron scattering by the disordered spin structure above T_N . The superconductivity sets in at $T=T_c^* \approx 6.6\text{ K}$ with the superconducting transition temperature $T_c=6.0\text{ K}$, defined as the temperature at which the steepest part of the resistance curve extrapolates to zero resistance. The transition width ΔT (90%–10% drop in the resistivity) is

TABLE I. Characteristic properties of single-crystal $R\text{Ni}_2\text{B}_2\text{C}$ compounds with $R=\text{Lu}, \text{Tm}, \text{Er}, \text{Ho},$ and Dy . T_c^* is the onset T_c ; l is determined from Eq. (1) in the text; λ_{tr} is determined from Eq. (2) in the text; λ is determined from Eq. (3) in the text using $T_c=T_c^*$ and $\mu^*=0.15$; ρ_0 , A , and p are determined from a least-squares fit of the low-temperature data to Eq. (6).

Rare earth	Dy	Ho	Er	Tm	Lu
T_c (K)	6	8.6	10.8	10.9	16.6 ^a
T_N (K)	10.5	5.2	5.9 ^b	1.5 ^c	
ρ_{RT} ($\mu\Omega$ cm)	41.6	43.7	47.8	49.8	46.8 ^a
$\rho(T_c^*)$ ($\mu\Omega$ cm)	1.8	4.0	3.8	4.2	1.9 ^a
$[d\rho/dT]_{\text{RT}}$ ($\mu\Omega$ cm/K)	0.13	0.15	0.15	0.16	0.15 ^a
l (eV \AA^3)	0.6	0.6 ^d	0.7		
$\Delta\rho_m$ ($\mu\Omega$ cm)	2.4	1.6 ^d	0.3–0.1 ^e		0
$l(\text{RT})$ (\AA)	8.6	8.3	7.6	7.3	7.6 ^a
$l(T_c^*)$ (\AA)	195	90	93	86	190 ^a
λ_{tr}	0.84	0.97	0.97	1.03	0.97 ^a
$\lambda(\mu^*=0.15)$	0.74	0.84	0.93	0.93	1.14 ^a
ρ_0 ($\mu\Omega$ cm)	4.01	3.96	3.55	3.53	1.36 ^a
A ($\mu\Omega$ cm/ K^{P^-})	2.6×10^{-5}	1.5×10^{-4}	2.2×10^{-3}	2.36×10^{-2}	$1.8 \times 10^{-3\text{a}}$
p	3.0	2.6	2.0	1.4	2.0 ^a
$S(\text{RT})$ ($\mu\text{V}/\text{K}$)	−10.9	−8.6	−8.7	−6.6	−7.3 ^a
ΔS_m ($\mu\text{V}/\text{K}$)	−0.8				
$[dS/dT]_{\text{RT}}$ (nV/ K^2)	−23.5	−19.0	−14.9	−13.8	−10.4 ^a
$(S - TdS/dT)_{\text{RT}}$ ($\mu\text{V}/\text{K}$)	−3.4	−3.0	−4.4	−2.7	−4.4 ^a

^aRef. 30.

^bRef. 6.

^cRef. 20.

^dRef. 5.

^eRef. 7.

≈ 0.5 K and is reasonably sharp, indicating the good quality (homogeneous) of the sample. The resistivity at T_N is $4.2 \mu\Omega$ cm, and at T_c^* is $1.8 \mu\Omega$ cm; thus, the decrease in the resistivity due to the antiferromagnetic ordering is $2.4 \mu\Omega$ cm, which is $\approx 0.7 \mu\Omega$ cm less than the decrease observed by Cho *et al.*⁷ The resistivity ratio (RR), defined as $\rho(295 \text{ K})/\rho(T_c^*)$, is 23 for the Dy sample, which is also indicative of the good quality of the sample.

The temperature-dependent behavior of the in-plane resistivity of the Ho, Er, and Tm samples is similar to that of the Dy sample, i.e., linear from ≈ 100 to 300 K, with a very

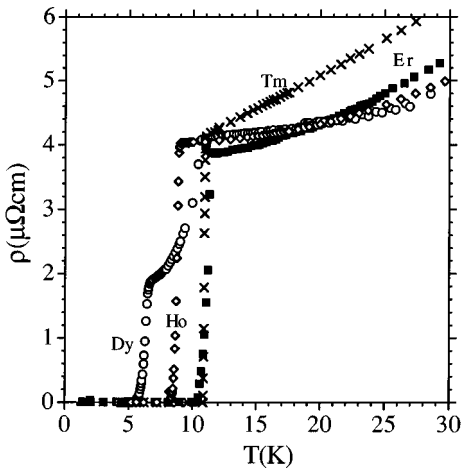


FIG. 2. Low-temperature data of Fig. 1.

small negative curvature at higher temperatures, and nonlinear below 100 K. The values of $[d\rho/dT]_{\text{RT}}$ for both the Ho and Er samples are $0.15 \mu\Omega$ cm/K and agree with the value reported by Cho *et al.*⁷ for the Er sample. The superconductivity sets in at $T=T_c^*=9.0, 11.4,$ and 11.2 K, respectively, with $T_c=8.6, 10.8,$ and 10.9 K, respectively, for the Ho, Er, and Tm samples. The resistivities of the Ho, Er, and Tm samples at T_c^* are almost twice that for the Dy sample at T_c^* (see Table I). The resistance ratios are $\text{RR} \approx 11, 13,$ and 12 for the Ho, Er, and Tm samples, respectively, almost one-half of the RR value of the Dy sample, and indicate that these samples have more imperfections and/or defects. However, the resistivity values at T_c^* for the Ho, Er, and Tm samples include the resistivity contribution due to spin disorder (ρ_{spd}) as the Néel temperatures of $\text{HoNi}_2\text{B}_2\text{C}$, $\text{ErNi}_2\text{B}_2\text{C}$, and $\text{TmNi}_2\text{B}_2\text{C}$ are below the superconducting transitions. One can estimate this resistivity contribution by applying a sufficiently large magnetic field to the sample which will reduce T_c below T_N . Rathnayaka *et al.*⁵ find $\Delta\rho \approx 1.6 \mu\Omega$ cm for $\text{HoNi}_2\text{B}_2\text{C}$. Cho *et al.*⁷ find that $\Delta\rho \approx 0.3 \mu\Omega$ cm for $\text{ErNi}_2\text{B}_2\text{C}$ if the applied magnetic field H is parallel to the c axis and that it is $< 0.1 \mu\Omega$ cm if H is perpendicular to the c axis. These values for the Er sample are more than 10 times smaller than the $\Delta\rho$ observed for the Dy and Ho samples. Values of $\Delta\rho$ for $\text{TmNi}_2\text{B}_2\text{C}$ with its $T_N \approx 1.5$ K have not been reported.

Based on the measured values of $\rho(\text{RT})$ and $[d\rho/dT]_{\text{RT}}$ of the Dy, Ho, Er, and Tm samples in this work, the electron mean free path (l) and the transport electron-phonon coupling parameter (λ_{tr}) are estimated from the relations⁵

$$\rho^{-1} = \frac{2}{3} e^2 N(0) v_F l, \quad (1)$$

$$\frac{d\rho}{dT} = \frac{8\pi^2}{\hbar \omega_p^2} k_B \lambda_{tr}, \quad (2)$$

where $N(0)$ is the density of states at the Fermi level, v_F is the Fermi velocity, and ω_p is the plasma frequency. The parameters $N(0)$, v_F , and ω_p are not available in the literature for any of the samples; therefore, values for these parameters calculated for $\text{LuNi}_2\text{B}_2\text{C}$,¹³ i.e., $N(0) = 4.8$ [states/eV unit cell], $v_F = (v_{Fx}^2 + v_{Fy}^2 + v_{Fz}^2)^{1/2} = 3.6 \times 10^7$ cm/s, and $\omega_p = 5.1$ eV are used to calculate l at T_c^* and at room temperature and λ_{tr} . The values are listed in Table I. The electron mean free path l at room temperature in these samples is of the order of their atomic spacing. Therefore, the standard Boltzmann theory is expected to break down at RT and higher temperatures. However, flattening of the resistivity with temperature is very small; therefore, the linearity between ρ and T near RT is assumed to be a valid assumption. The calculated values of λ_{tr} for Dy, Ho, Er, and Tm from Eq. (2) are reasonable and compare well with values of λ_{tr} similarly calculated for $\text{LuNi}_2\text{B}_2\text{C}$.³⁰ Thus they represent a semi-empirical measure of the electron-phonon coupling constant λ , which appears in the McMillan equation for the superconducting transition temperature T_c . With the knowledge of T_c and Debye temperature Θ_D of a superconductor, λ can be estimated from the McMillan equation³⁴

$$k_B T_c = \frac{\hbar \omega_{\log}}{1.2} \exp \left[- \frac{1.04(1+\lambda)}{\lambda - \mu^*(1+0.62\lambda)} \right], \quad (3)$$

where ω_{\log} is taken to be $0.7 \omega_{ph}$, ω_{ph} is regarded to be the same as $\omega_D = k_B \Theta_D / \hbar$, and μ^* is the Coulomb pseudopotential and usually taken to be between 0.1 and 0.15. Debye temperatures for these compounds have not yet been reported; therefore, the Debye temperature of $\text{LuNi}_2\text{B}_2\text{C}$ (345 K) (Ref. 35) is used with appropriate mass scaling, i.e., $\Theta_D(\text{Dy}) = \Theta_D(\text{Lu}) \{M(\text{Lu})/M(\text{Dy})\}^{1/2}$, where $M(\text{Lu})$ and $M(\text{Dy})$ are the atomic masses of Lu and Dy, respectively. This scaling yields $\Theta_D(\text{Dy}) \approx 358$ K, $\Theta_D(\text{Ho}) \approx 355$ K, $\Theta_D(\text{Er}) \approx 353$ K, and $\Theta_D(\text{Tm}) \approx 351$ K. Values of λ calculated from Eq. (3) with $\mu^* = 0.15$ and T_c^* used as T_c are tabulated in Table I. If T_c values are used, then values of λ decrease by about 0.02 for Dy, 0.04 for Ho, 0.03 for Er, and 0.03 for Tm. Use of T_c or T_c^* clearly neglects a proper accounting for pair-breaking effects due to magnetic scattering in these alloys. While $\lambda(\text{Er})$ agrees reasonably well with $\lambda_{tr}(\text{Er})$, the agreement between values of λ and λ_{tr} for the Dy, Ho, and Tm samples is not so good. However, a 10–15 % disagreement between λ_{tr} and λ is commonly found in other superconductors³⁶ without magnetic ions. The range of λ_{tr} or λ values for the Dy, Ho, Er, and Tm samples estimated in this work shows that these compounds are also moderately strong-coupling superconductors like Y/LuNi₂B₂C. A comparison of these compounds with some A-15 superconductors which have T_c near 15 K, i.e., Nb₃Sn ($T_c \approx 17$ K), V₃Si ($T_c \approx 15$ K), show that λ values of DyNi₂B₂C, ErNi₂B₂C, and TmNi₂B₂C superconductors are close to that of V₃Si ($\lambda \approx 1.0$) and much smaller than those of Nb₃Sn

($\lambda \approx 1.8$) and Nb₃Al ($\lambda \approx 1.5$).³⁷ The strong-coupling elemental superconductors Pb and Nb have $\lambda \approx 1.5$ and 1.0, respectively.³⁶

In the normal state, the resistivity of the sample can be expressed as the sum of the residual resistivity, that due to electron-phonon scattering and that from the magnetic scattering by disordered spins, i.e.,

$$\rho_{\text{total}} = \rho_0 + \rho_{\text{ph}} + \rho_{\text{spd}}. \quad (4)$$

The exchange constant I between the conduction electrons and the R^{3+} ions can be estimated from the contribution to the resistivity by spin disorder scattering ρ_{spd} according to the relation³⁸

$$\rho_{\text{spd}} = \frac{3\pi N}{\hbar e^2 v_F^2} I^2 (g-1)^2 J(J+1), \quad (5)$$

where N is the number of rare-earth atoms per unit volume, v_F the Fermi velocity, g the Lande g factor, and J the total angular momentum of the localized rare-earth ion in units of \hbar . The exchange constant I is calculated from the measured value of the abrupt drop in resistivity ($\Delta\rho = \rho_{\text{spd}}$) at the Néel temperature for the Dy, Ho, and Er samples, with v_F taken to be the same as for $\text{LuNi}_2\text{B}_2\text{C}$. The values of the exchange constant I are 0.6, 0.6, and 0.7 eV Å³ from Eq. (5), respectively, for the Dy, Ho, and Er samples, or, equivalently, ρ_{spd} for these three samples obeys de Gennes scaling (see Ref. 38 and references therein). Similar results were reported for $R\text{Al}_2$ compounds.³⁸ The almost identical values of I indicate that there is no significant difference in the magnetic interactions between the conduction electrons and the R^{3+} ions, in these samples, yet quite different magnetic behavior is observed for each of the three. We note that T_N also exhibits de Gennes scaling; i.e., T_N is proportional to the de Gennes factor $(g-1)^2 J(J+1)$.^{7,10}

Although the in-plane resistivity of each sample varies approximately linearly with temperature near room temperature, as expected for a good metal, it shows nonlinearity with temperature below 100 K and does not decrease as rapidly as expected from the conventional Bloch-Grüneisen theory. A similar observation has been reported³⁰ for YNi₂B₂C and LuNi₂B₂C. To determine the exact temperature dependence of $\rho(T)$, the low-temperature data for all four samples were fitted to the power-law expression

$$\rho(T) = \rho_0 + AT^p, \quad (6)$$

in the temperature interval $1.25T_c^*$ (or $1.2T_N$ if $T_N > T_c^*$) $< T < 0.1\Theta_D$ using a least-squares fit procedure, with the square of the correlation coefficient determining the goodness of the fit. The temperature region above $1.25T_c$ for the Ho, Er, and Tm samples, and $1.2T_N$ for the Dy sample, was chosen to minimize the superconducting-magnetic fluctuation effects. The in-plane ρ_0 , A , and p parameters obtained from the fit are given in Table I. Figure 3 shows ρ vs $T^{2.6}$ for the Ho sample, displaying the typical good fit obtained from Eq. (6). The present results show that the in-plane resistivity of Ho/Er/TmNi₂B₂C layered compounds does not follow the T^5 or T^3 dependence at low temperatures usually observed for normal and transition metals. The in-plane resistivity of the DyNi₂B₂C sample shows a T^3 dependence and is consis-

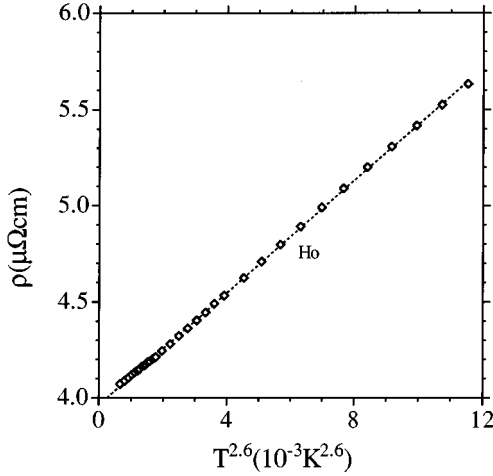


FIG. 3. Resistivity ρ vs $T^{2.6}$ for $\text{HoNi}_2\text{B}_2\text{C}$ over the temperature range $1.25T_c$ to $0.1\Theta_D$.

tent with phonon scattering. The exponent p is close to 3 for the Ho sample, but it is quite different ($p \approx 2$) for the Er sample, which is similar to the p value observed for $\text{Y/LuNi}_2\text{B}_2\text{C}$,³⁰ and disordered, strong-coupling A-15 intermetallic compounds.³⁷ It is expected that the crystal-field splitting, interband transitions, and other complexities in the electronic structure of these compounds may produce some temperature dependence in the scattering at higher temperatures, resulting in a modified temperature dependence of the resistivity. The constants A for the Dy/Ho/Er/Tm $\text{Ni}_2\text{B}_2\text{C}$ samples differ by an order of magnitude, i.e., $A(\text{Tm})/A(\text{Er}) \approx 10$, $A(\text{Er})/A(\text{Ho}) \approx 10$, and $A(\text{Ho})/A(\text{Dy}) \approx 10$. The constant A for Ho is of the same order of magnitude as found for $\text{Y/LuNi}_2\text{B}_2\text{C}$,^{28,30} but the coefficient A for Er, which shows the same T^2 dependence as Y and Lu, is an order of magnitude larger than that for these two compounds. The constant A (as well as the exponent p) is quite sensitive to the temperature interval used to fit the data to Eq. (6). Therefore, it is necessary that the fitting temperature interval be stated explicitly for the determination of the constant A as well as p , which has been done clearly in this work. (Values for ρ_0 and A for $\text{TmNi}_2\text{B}_2\text{C}$ are incorrectly printed in Ref. 28, but the value p is correctly given.) Thus the temperature dependence of electrical resistivity of $\text{RNi}_2\text{B}_2\text{C}$ ($R = \text{Y, Lu, Ho, Er, Tm}$) layered compounds, in the temperature interval $1.25T_c^*$ (or T_N if $T_N > T_c^*$) $< T < 0.1\Theta_D$, does not follow the predictions of the conventional theories for simple normal or transition metals. The resistivity of high- T_c A-15 intermetallic compounds and highly disordered metallic systems, whether superconducting, magnetic, or normal, has been found to vary as $\approx T^2$, similar to that observed for Er/Y/Lu $\text{Ni}_2\text{B}_2\text{C}$ single crystals. Gurvitch³⁹ has proposed that strong electron-phonon coupling together with high disorder can explain the T^2 dependence in the A-15's and disordered alloys; however, the samples investigated here and earlier^{28,30} are not highly disordered, although they are layered compounds and moderately strong-coupling superconductors. A T^2 dependence is also associated with an electron-electron scattering mechanism, but the fact that the coefficient A for Er is an order of magnitude larger than the value for Y or Lu, which is already two to three orders of

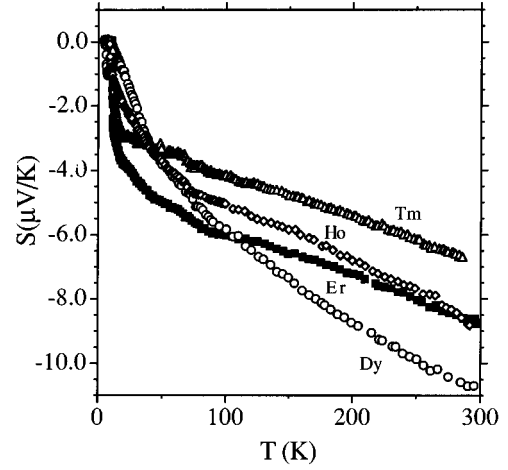


FIG. 4. Thermopower S of $\text{DyNi}_2\text{B}_2\text{C}$, $\text{ErNi}_2\text{B}_2\text{C}$, $\text{HoNi}_2\text{B}_2\text{C}$, and $\text{TmNi}_2\text{B}_2\text{C}$ single crystals as a function of temperature. Symbols are the same as in Fig. 1.

magnitude larger than that expected for electron-electron scattering,³⁰ rules out that mechanism for the magnetic superconductor $\text{ErNi}_2\text{B}_2\text{C}$.

B. Thermopower

Figure 4 shows the in-plane absolute thermopower $S(T)$ as a function of temperature for the single crystals of $\text{DyNi}_2\text{B}_2\text{C}$, $\text{HoNi}_2\text{B}_2\text{C}$, $\text{ErNi}_2\text{B}_2\text{C}$, and $\text{TmNi}_2\text{B}_2\text{C}$ from RT to 4 K. Figure 5 shows $S(T)$ vs T below 20 K to display the detailed behavior of the thermopowers near the superconducting transition temperatures. The absolute thermopower is negative for all the three samples from RT to just above T_c at which it rapidly falls to zero within the measurement accuracy. T_c determined this way is within ± 0.5 K of that determined by the resistivity measurements. The sharp fall of S to zero at T_c also confirms the good quality of the samples. While the temperature behavior of the thermopower of $\text{HoNi}_2\text{B}_2\text{C}$, $\text{ErNi}_2\text{B}_2\text{C}$, and $\text{TmNi}_2\text{B}_2\text{C}$ near T_c is similar to other $\text{RNi}_2\text{B}_2\text{C}$ ($R = \text{Y, Lu}$) superconductors,³⁰ the Dy sample shows strikingly different behavior in the tempera-

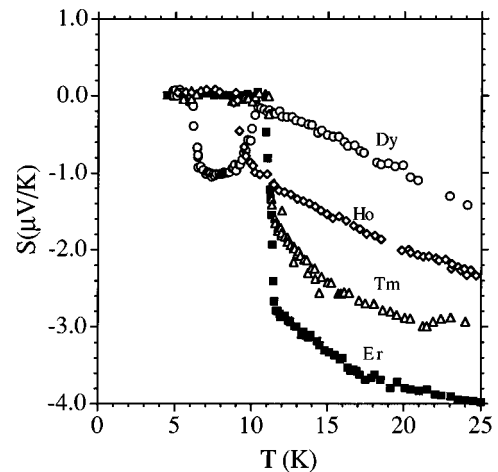


FIG. 5. Low-temperature data from Fig. 4.

ture region $T_c < T < T_N$ (Fig. 5). At $T \approx 10.4$ K, $S(T)$ suddenly increases in magnitude (remaining negative though) and produces a kink at this temperature in S vs T data. The net change in $S(T)$ is $\approx 0.8 \mu\text{V/K}$ before it abruptly falls to zero at T_c (≈ 6.0 K). The temperature $T \approx 10.4$ K is identified as the Néel temperature T_N at which the antiferromagnetic ordering takes place and agrees with the temperature at which the sharp drop in the resistivity occurs. The increase in the magnitude of the thermopower below T_N is related to the contribution from the ordered antiferromagnetic magnetic state of the crystal. Similar behavior has been observed in other antiferromagnetic metallic systems, e.g., thulium single crystals.⁴⁰ The Ho and Er samples do not show this striking change in the thermopower (or the resistivity) because their Néel temperatures [$T_N(\text{Ho}) \approx 5$ K and $T_N(\text{Er}) \approx 6.8$ K] are smaller than their superconducting transition temperatures T_c . The negative thermopower for all the three samples suggests that the charge carriers in these compounds are in all likelihood electrons, in agreement with the band structure calculations^{12–14} on the similar borocarbide compound $\text{LuNi}_2\text{B}_2\text{C}$.

The thermopower of these samples is linear in T near room temperature within the measurement accuracy similar to free-electron-like behavior. Room-temperature values of thermopower $S(\text{RT})$ are given in Table I. The magnitude of $S(\text{RT})$ is about the same as that of some transition metals like palladium, but it is somewhat larger than the typical value associated with free electron and conventional metals, which is not surprising since Ni is a major constituent of the compounds and Ni $3d$ bands mainly determine the electronic behavior of these compounds.

The extrapolation of the $S(T)$ data near room temperature, assuming a linear T dependence of S , does not pass through $S=0$ at $T=0$ and gives large intercepts. These intercepts depend somewhat upon the exact temperature interval between 100 and 300 K in which $S(T)$ is fitted, i.e., but the intercepts for fitting the different intervals for a given sample agree within 5%. The data in the temperature region between 125 K and RT were fitted to a straight line for all four samples. The intercepts are -3.79 , -2.99 , -4.29 , and $-2.67 \mu\text{V/K}$, respectively, for the Dy, Ho, Er, and Tm samples. The intercept value for the Er sample is strikingly similar to that reported for single crystals of $\text{YNi}_2\text{B}_2\text{C}$ ($-4.61 \mu\text{V/K}$) and $\text{LuNi}_2\text{B}_2\text{C}$ ($-4.34 \mu\text{V/K}$) samples,³⁰ although the Y/LuNi₂B₂C samples are nonmagnetic while the Er sample becomes magnetic at low temperatures, i.e., the scattering contributions from the spin disorder as well as crystal field splitting seem to be either absent or too small to make any difference between the intercepts for the ErNi₂B₂C and Y/LuNi₂B₂C samples. The intercept values for the Dy, Ho, and Tm samples are smaller than those for Er/Y/LuNi₂B₂C single crystals, with the intercept for the Ho sample being about 30% smaller than that for sc-Er/Y/LuNi₂B₂C samples.³⁰ Similar intercepts in S vs T have been observed for high- T_c cuprates⁴¹ as well as for amorphous metals.⁴² Although the reported magnitude of such an intercept in amorphous metals is much smaller, it can be as large in high- T_c cuprates as that observed for single crystals of $\text{RNi}_2\text{B}_2\text{C}$.³⁰

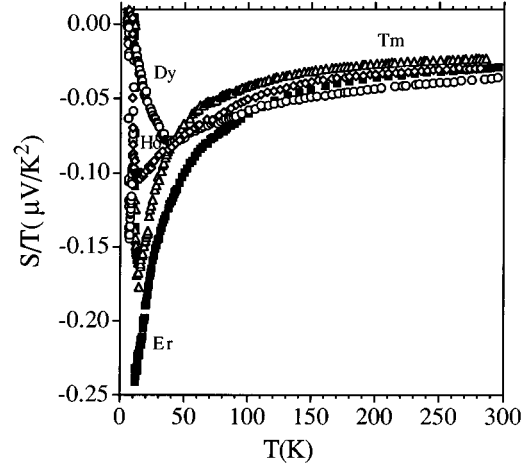


FIG. 6. S/T as a function of temperature for $\text{DyNi}_2\text{B}_2\text{C}$, $\text{ErNi}_2\text{B}_2\text{C}$, $\text{HoNi}_2\text{B}_2\text{C}$, and $\text{TmNi}_2\text{B}_2\text{C}$ single crystals. Symbols are the same as in Fig. 1.

In free-electron-like metals, the diffusion thermopower which is proportional to T should be the major contribution to the total thermopower. For magnetic compounds the Nordheim-Gorter rule gives³⁸

$$S = (\rho_0/\rho)S_0 + (\rho_{\text{ph}}/\rho)S_{\text{ph}} + (\rho_{\text{spd}}/\rho)S_{\text{spd}}, \quad (7)$$

where S_0 , S_{ph} , and S_{spd} are the contributions to the thermopower due to impurity scattering, scattering by phonons, and spin-disorder scattering, respectively. ρ , ρ_0 , ρ_{ph} , and ρ_{spd} represent the total resistivity, the residual resistivity, the resistivity due to phonon scattering, and that due to spin-disorder scattering, respectively. In GdAl_2 , GdCu_2 , and GdNi_2 , the spin-disorder scattering contribution determined from a Nordheim-Gorter analysis was found to be linear in temperature above the ordering temperature.³⁸ Although this is not always the case observed for magnetic impurities, one might expect a magnetic contribution that is linear in T for these compounds. Other mechanisms can change the temperature dependence of the thermopower from linear to non-linear assuming that the linear part arises only from the diffusion or magnetic contribution to the thermopower. There are always other contributions in pure metals, one of which is the phonon drag contribution. A plot of S/T vs T as in Fig. 6 is often useful in identification of the additional contributions. In Fig. 6, $[S/T]$ vs T data for the Er and Ho samples almost overlap at higher temperatures ($T > 100$ K) and those for the Dy and Ho samples are not very different either in the same temperature range. At lower temperature the similarity between the data is much less, even though all show a negative peak in the data, with Dy showing a second negative peak between T_N and T_c . The shape of this peak for the Er sample is very similar to that observed for Y/LuNi₂B₂C,³⁰ which is quite surprising since the rare-earth-nickel borocarbides with Y and Lu are completely nonmagnetic. The magnitude of the negative peaks for the Tm, Ho, and Dy compounds are much less than that for Er, and the peak temperature for Dy (high- T peak) is much larger than for the other three compounds. The usual phonon drag contribution for metals falls at low temperature as the phonons freeze out and at high temperatures as the excess phonon momentum

gets limited by phonon-phonon scattering. Typically, the phonon drag peak in conventional metals shows a T^3 dependence below $0.1 \Theta_D$ and falls as T^{-1} above $\approx 0.3 \Theta_D$; i.e., at low and high temperatures, the diffusion thermopower becomes the dominant contribution to the total thermopower. Since the samples are single crystals with relatively low resistivities, such behavior should be expected. The data presented in Figs. 4 and 6 do not exhibit this typical behavior, indicating that the phonon drag peak is either absent, too small to be identified, or shows a much different temperature behavior (to be discussed further below). The S/T curves are instead similar to those for amorphous alloys⁴² or, except for sign, many high- T_c cuprate superconductors.⁴¹

The shape of the $[S/T]$ vs T data for the samples is similar to that associated with electron-phonon renormalization effects.⁴³ Electron-phonon renormalization leads to an enhanced thermopower that is given by

$$S = S_b [1 + \lambda(T)], \quad (8)$$

where $\lambda(T)$ is the electron-phonon mass enhancement parameter and S_b is the bare thermopower (without renormalization effects). In this expression certain other corrections have been ignored which are relatively small and can be ignored as a first approximation.⁴⁴ Equation (8) is rewritten as

$$\frac{S}{T} = \frac{S_b}{T} [1 + \lambda(T)], \quad (9)$$

where $\lambda(T)$, the electron-phonon mass enhancement parameter, is maximum at $T=0$ K and becomes smaller as T is raised, becoming almost negligible near RT and higher temperatures in comparison with 1. A plot of $[S/T]$ vs T should, therefore, give a measure of $\lambda(T)$, and $[S/T]_{T \rightarrow 0}/[S/T]_{RT}$ should approximate $1 + \lambda(0)$. Due to the onset of superconductivity and/or magnetic order, it is difficult to determine the ratio $[S/T]_{T \rightarrow 0}/[S/T]_{RT}$ precisely. However, to get some *qualitative* feeling as to the importance of these renormalization effects in $S(T)$ for these compounds, the $[S/T]$ value just above T_c is taken to be $[S/T]_{T \rightarrow 0}$ as an approximation for the Tm, Er, and Ho samples. Using these values of $[S/T]_{T \rightarrow 0}$ and values of $[S/T]_{RT}$ from Fig 6, estimated values of $\lambda(0)$ are approximately 7.5, 4.0, and 2.5, respectively, for the Er, Tm, and Ho samples, respectively. The value of $\lambda(0)$ for the Er sample is similar to the one found for Y/LuNi₂B₂C single crystals from a similar analysis of $[S/T]$ data³⁰ and is unrealistically high in comparison with the values of $\lambda(0)$ for conventional superconductors including strong-coupling ones or to those obtained here either from the resistivity data, λ_{lr} , or the McMillan equation (3), $\lambda(\mu^* = 0.15)$. The same difficulty arises with the estimate of $\lambda(0)$ for the Tm and Ho samples, although they are about one-half to one-third of that for the Er/Y/LuNi₂B₂C single crystals. A similar difficulty seems to exist in the interpretation of the thermopower data of high- T_c cuprates,⁴¹ although Kaiser and Mountjoy⁴⁵ have shown that the thermopower of high- T_c superconductors can be explained within the existing metallic diffusion-thermopower theory if an anomalously large electron-phonon coupling (greater than 5) is assumed to exist, such as might arise from an anharmonic double-well potential⁴⁶ in YBa₂Cu₃O_{7- δ} .

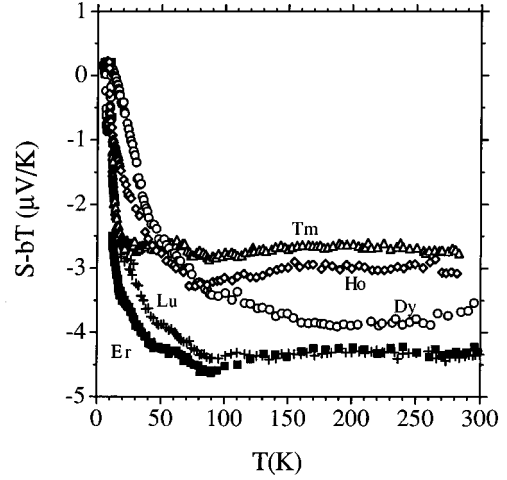


FIG. 7. $S(T)-bT$ as a function of temperature for DyNi₂B₂C, ErNi₂B₂C, HoNi₂B₂C, and TmNi₂B₂C single crystals. The plusses (+) represent the data for LuNi₂B₂C from Ref. 30. Symbols are the same as in Fig. 1.

Since all four samples show antiferromagnetic behavior at some low temperature, one might expect spin fluctuations to be present in these materials. In such a case, Eq. (8) is modified to

$$\frac{S}{T} = \frac{S_b}{T} [1 + \lambda(T) + \lambda_{sf}], \quad (10)$$

where λ_{sf} is the mass enhancement parameter due to spin fluctuations. Neutron-diffraction measurements on ErNi₂B₂C (Ref. 47) suggest the possibility of an ordered magnetic moment on the Ni atom in the antiferromagnetic state, and the possibility of the existence of dynamically fluctuating moments in Ni was reported for TmNi₂B₂C.⁴⁸ However, λ_{sf} is not expected to have sufficiently large values which could explain $[S/T]_{T \rightarrow 0}/[S/T]_{RT} \approx 6-8$. Consequently, electron-phonon renormalization effects do not explain the $S(T)$ data for these compounds.

It is clear that there is an additional term present for these four compounds beyond the term linear in T . This additional term does not fit the behavior commonly associated with phonon drag in metals or electron-phonon mass renormalization. To determine the contribution other than the “diffusion-magnetic” contribution which is proportional to T , $(S-bT)$ vs T for Dy/Ho/Er/TmNi₂B₂C single crystals is plotted in Fig. 7, where b is the coefficient obtained by fitting the S vs T data to a straight line, i.e., $S(T) = a + bT$, in the linear region ($T \approx 125$ K to RT). $(S-bT)$ represents contributions to the thermopower other than the diffusion thermopower (and any other contribution which may be proportional to T). The surprising result of Fig. 7 is that this negative contribution is almost constant between 100 and 300 K for the Ho/Er/Tm samples. $(S-bT)$ for Dy shows a very weak temperature dependence in this range. Also quite surprising is the fact that $(S-bT)$ for the Er sample is practically identical to that found for Y/LuNi₂B₂C,³⁰ both in magnitude and in temperature dependence, as shown in Fig. 7 where the data for the Lu sample are also included for comparison. Values of $b = [dS/dT]_{RT}$ and $(S-bT)_{RT}$ at

room temperature are included in Table I. Below 100 K, this contribution ($S - bT$) to the thermopower for the Ho, Er, and Dy samples varies approximately as $(S_0 + c/T)$, until the superconducting transition temperature at which it drops suddenly to zero for the Ho and Er samples, while in case of the Dy sample the onset of the magnetic order changes the temperature dependence drastically below T_N . For the Tm sample, $(S - bT)$ is approximately constant down to about 40 K where it increases sharply.

From a conventional view this almost constant contribution ($S - bT$) is quite puzzling. Any contribution from possible magnetic impurities is expected to be much smaller than that observed in Fig. 7. Recently, Trodahl⁴⁹ has proposed that the unusual temperature dependence of the thermopower of high- T_c cuprate superconductors results from the phonon drag contribution, but with the assumption that the phonon-phonon scattering in high- T_c cuprates remains weaker than phonon-electron scattering, even at room temperature. He finds that the temperature dependence of the phonon drag contribution to the thermopower of the high- T_c cuprates is very similar to that shown in Fig. 6; i.e., it is almost temperature independent between 100 K and RT, and this constant value represents the saturation value of the phonon drag thermopower. This kind of temperature dependence of the phonon drag thermopower leads to a simple shift of the linear diffusion thermopower between 100 K and RT. This particular behavior relates to the layered nature of high- T_c cuprates. Although the rare-earth-nickel borocarbides are also layered compounds physically, it is thought that both the electronic structure and the phonon behavior should be quite isotropic. Nevertheless, the possibility that $(S - bT)$ in Fig. 7 is primarily due to phonon drag with the phonon-phonon scattering remaining much weaker at room temperature than electron-phonon scattering for these compounds is intriguing.

Most surprising is that there is no clear magnetic signature, beyond the small increase $0.8 \mu\text{V/K}$ in the magnitude of S for Dy just below T_N and the rather strong variation in the magnitude of the “diffusion-magnetic” term bT where $b = [dS/dT]_{\text{RT}}$ more than doubles in going from Lu to Dy. The coefficient b also scales with the de Gennes factor. Most analyses of experimental data on these borocarbides have assumed that the electronic structure is essentially the same as that of Y or Lu for all of the rare earths. Thus, except for scattering from magnetic impurities, the diffusion thermopowers should be identical in the high-temperature range. The Nordheim-Gorter rule [Eq. (7)] provides an explanation of the scaling of the coefficient b with the de Gennes factor since ρ_{spd} also scales by the same factor. It does not, how-

ever, explain the small increase in magnitude of S for Dy at T_N , which is perhaps related to a change in the electronic structure due to magnetic ordering.

IV. SUMMARY AND CONCLUSIONS

In-plane transport measurements for the $R\text{Ni}_2\text{B}_2\text{C}$ intermetallics which exhibit the coexistence of superconducting and magnetic order at low temperature ($R = \text{Dy-Tm}$) indicate many similarities with transport in the comparable intermetallics which show superconductivity without magnetic order ($R = \text{Y, Lu}$), but they also show important differences. The behavior of the high-temperature resistivity is very similar to a comparable room-temperature coefficient of resistivity, $\text{TCR} = \rho^{-1} d\rho/dT$, resistivity ρ , and transport electron-phonon coupling constant λ_{tr} . The low-temperature behavior of ρ can be described by $\rho = \rho_0 + AT^p$, with $1.4 \leq p \leq 3$. The temperature dependence of the thermopower can be described by two terms, a linear “diffusion-magnetic” contribution term bT and a second contribution $S - bT$, which is very similar for the compounds with $R = \text{Y, Lu, Tm-Dy}$. The coefficient b increases systematically from $b = -10.4 \text{ nV/K}^2$ for $R = \text{Lu}$ to $b = -23.5 \text{ nV/K}^2$ for $R = \text{Dy}$, scaling with the de Gennes factor. Consequently, these variations in b appear to be related to the magnetic scattering. The remaining term $S - bT$ is approximately independent of temperature from room temperature to 150 K for all of the compounds with a similar magnitude, -2.5 to $-4.8 \mu\text{V/K}$, indicating that it does not arise primarily from magnetic scattering. To our knowledge this is the first system of intermetallic compounds to show such a large, relatively temperature-independent contribution to the thermopower up to room temperature. A possible explanation would be saturation of the phonon drag contribution as proposed by Trodahl⁴⁹ for high- T_c cuprates. The similarity between transport in the magnetic superconductor with $R = \text{Er}$ and the non-magnetic superconductors ($R = \text{Y, Lu}$) is remarkable with an identical T^2 temperature dependence of the resistivity at low temperature and essentially identical second contributions ($S - bT$) to the thermopower over the entire temperature range above T_c : i.e., the only difference is essentially the larger value of b .

ACKNOWLEDGMENTS

Work at Texas A&M was supported by the Robert A. Welch Foundation (Grant No. A-0514). Ames Laboratory is operated for the U.S. Department of Energy by the Iowa State University under Contract No. W-7405-ENG-82. The work at Ames was supported by the Director for Energy Research, Office of Basic Energy Sciences.

¹T. Siegrist, H. W. Zandbergen, R. J. Cava, J. J. Krajewski, and W. F. Peck, Jr., *Nature (London)* **367**, 254 (1994).

²T. Ekino, H. Fujii, M. Kosugi, Y. Zenitani, and J. Akimitsu, *Phys. Rev. B* **53**, 5640 (1996).

³M. B. Maple and Ö Fischer, *Superconductivity in Ternary Compounds III* (Springer-Verlag, Berlin, 1982), and references therein.

⁴H. Eisaki, H. Takagi, R. J. Cava, B. Batlogg, J. J. Krajewski, W.

F. Peck, Jr., K. Mizuhashi, J. O. Lee, and S. Uchida, *Phys. Rev. B* **50**, 647 (1994).

⁵K. D. D. Rathnayaka, D. G. Naugle, B. K. Cho, and P. C. Canfield, *Phys. Rev. B* **53**, 5688 (1996).

⁶B. K. Cho, P. C. Canfield, L. L. Miller, D. C. Johnston, W. P. Beyermann, and A. Yatskar, *Phys. Rev. B* **52**, 3684 (1995).

⁷B. K. Cho, P. C. Canfield, and D. C. Johnston, *Phys. Rev. B* **52**, R3844 (1995).

- ⁸B. K. Cho, M. Xu, P. C. Canfield, L. L. Miller, and D. C. Johnston, *Phys. Rev. B* **52**, 3676 (1995).
- ⁹B. K. Cho, P. C. Canfield, and D. C. Johnston, *Phys. Rev. B* **53**, 8499 (1996); C. V. Tomy, L. A. Afalfiz, M. R. Lees, J. M. Martin, D. McK. Paul, and D. T. Adroja, *ibid.* **53**, 307 (1996).
- ¹⁰P. C. Canfield, B. K. Cho, and K. W. Dennis, *Physica B* **215**, 337 (1995).
- ¹¹S. K. Dhar, R. Nagarajan, Z. Hossain, E. Tominez, C. Godart, L. C. Gupta, and R. Vijayaraghavan, *Solid State Commun.* **98**, 985 (1996); A. Yatskar, N. K. Budraa, W. P. Beyermann, P. C. Canfield, and S. Bud'ko, *Phys. Rev. B* **54**, 3772 (1996).
- ¹²L. F. Mattheiss, *Phys. Rev. B* **49**, 13 279 (1994).
- ¹³W. E. Pickett and D. J. Singh, *Phys. Rev. Lett.* **72**, 3702 (1994).
- ¹⁴J. I. Lee, T. S. Zhao, I. G. Kim, B. I. Min, and S. J. Youn, *Phys. Rev. B* **50**, 4030 (1994).
- ¹⁵H. Kim, C. Hwang, and J. Ihm, *Phys. Rev. B* **52**, 4592 (1995).
- ¹⁶N. M. Hong, H. Michor, M. Vybornov, T. Holubar, P. Hundegger, W. Perthold, G. Hilscher, and P. Rogl, *Physica C* **227**, 85 (1994).
- ¹⁷S. A. Carter, B. Batlogg, R. J. Cava, J. J. Krajewski, W. F. Peck, Jr., and H. Takagi, *Phys. Rev. B* **50**, 4216 (1994).
- ¹⁸L. F. Rybaltchenko, I. K. Yanson, A. G. M. Jansen, P. Mandal, P. Wyder, C. V. Tomy, and D. McK. Paul, *Europhys. Lett.* **33**, 483 (1996); *Physica B* **218**, 189 (1996).
- ¹⁹S. A. Carter, B. Batlogg, R. J. Cava, J. J. Krajewski, W. F. Peck, Jr., and H. Takagi, *Phys. Rev. B* **50**, 4216 (1994).
- ²⁰R. Movshovich, M. F. Hundley, J. D. Thompson, P. C. Canfield, B. K. Cho, and A. V. Chubukov, *Physica C* **227**, 381 (1994).
- ²¹C. Godart, L. C. Gupta, R. Nagarajan, S. K. Dhar, H. Noel, M. Potel, C. Mazumdar, Z. Hossain, C. Levy-Clement, G. Schiffrmacher, B. D. Padalia, and R. Vijayaraghavan, *Phys. Rev. B* **51**, 489 (1995).
- ²²M. E. Hanson, F. Lefloch, W. H. Wong, W. G. Clark, M. D. Lan, C. C. Hoellwarth, P. Klavins, and R. N. Shelton, *Phys. Rev. B* **51**, 674 (1994).
- ²³S. Oxx, D. P. Choudhury, B. A. Willemsen, H. Srikanth, S. Sridhar, B. K. Cho, and P. C. Canfield, *Physica C* **264**, 103 (1996); T. Jacobs, B. A. Willemsen, S. Sridhar, R. Nagarajan, L. C. Gupta, Z. Hossain, C. Mazumdar, B. K. Cho, and P. C. Canfield, *Phys. Rev. B* **52**, R7022 (1995).
- ²⁴P. C. Canfield, B. K. Cho, D. C. Johnston, D. K. Finnemore, and M. F. Hundley, *Physica C* **230**, 397 (1994).
- ²⁵A. I. Goldman, C. Stassis, P. C. Canfield, J. Zarestky, P. Dervenagas, B. K. Cho, D. C. Johnston, and B. Sternlieb, *Phys. Rev. B* **50**, 9668 (1994).
- ²⁶P. Dervenagas, J. Zarestky, C. Stassis, A. I. Goldman, P. C. Canfield, and B. K. Cho, *Physica B* **212**, 1 (1995).
- ²⁷J. Zarestky, C. Stassis, A. I. Goldman, P. C. Canfield, P. Dervenagas, B. K. Cho, and D. C. Johnston, *Phys. Rev. B* **51**, 678 (1995).
- ²⁸K. D. D. Rathnayaka, A. K. Bhatnagar, D. G. Naugle, P. C. Canfield, and B. K. Cho, *Physica B* **223&224**, 83 (1996).
- ²⁹D. G. Naugle, K. D. D. Rathnayaka, A. K. Bhatnagar, A. C. Du Mar, A. Parasiris, J. M. Bell, P. C. Canfield, and B. K. Cho, *Czech. Phys.* **46**, Suppl. 6, 3263 (1966).
- ³⁰K. D. D. Rathnayaka, A. K. Bhatnagar, A. Parasiris, D. G. Naugle, P. C. Canfield, and B. K. Cho, *Phys. Rev. B* **55**, 8506 (1997).
- ³¹J. H. Lee, Y. S. Ha, Y. S. Song, Y. W. Park, and Y. S. Choi, in *Proceedings of the 10th Anniversary HTS Workshop in Physics, Materials and Applications*, edited by B. Batlogg, C. W. Chu, W. K. Chu, D. U. Gubser, and K. A. Müller (World Scientific, Singapore, 1996), pp. 332–334.
- ³²M. Xu, P. C. Canfield, J. E. Ostenson, D. K. Finnemore, B. K. Cho, Z. R. Wang, and D. C. Johnston, *Physica C* **227**, 321 (1994).
- ³³C. V. Tomy, M. R. Lees, G. Balakrishnan, D. T. Adroja, and D. McK. Paul, *Physica B* **223&224**, 62 (1996), and references therein.
- ³⁴W. L. McMillan, *Phys. Rev.* **167**, 331 (1968).
- ³⁵J. S. Kim, W. W. Kim, and G. R. Stewart, *Phys. Rev. B* **50**, 3485 (1994); S. A. Carter, B. Batlogg, R. J. Cava, J. J. Krajewski, W. F. Peck, Jr., and H. Takagi, *ibid.* **50**, 4216 (1994).
- ³⁶P. B. Allen, *Phys. Rev. B* **36**, 2920 (1987).
- ³⁷T. P. Orlando, E. J. McNiff, Jr., S. Foner, and M. R. Beasley, *Phys. Rev. B* **19**, 4545 (1979), and references therein.
- ³⁸E. Gratz and M. Zukermann, in *Handbook of the Physics and Chemistry of Rare Earths*, edited by K. A. Gschneider, Jr. and L. Eyring (North-Holland, Amsterdam, 1982), p. 138.
- ³⁹M. Gurvitch, *Phys. Rev. Lett.* **56**, 647 (1986).
- ⁴⁰L. R. Edwards and S. Legvold, *Phys. Rev.* **176**, 753 (1968); R. D. Barnard, *Thermoelectricity in Metals and Alloys* (Taylor & Francis, New York, 1972), Chap. 7.
- ⁴¹A. B. Kaiser and C. Uher, in *Studies of High Temperature Superconductors*, edited by A. V. Narlikar (Nova, New York, 1991), Vol. 7.
- ⁴²M. A. Howson and B. L. Gallagher, *Phys. Rep.* **170**, 265 (1988).
- ⁴³A. B. Kaiser, *Phys. Rev. B* **35**, 4677 (1987).
- ⁴⁴A. B. Kaiser and G. E. Stedman, *Solid State Commun.* **54**, 91 (1985).
- ⁴⁵A. B. Kaiser and G. Mountjoy, *Phys. Rev. B* **43**, 6266 (1991).
- ⁴⁶R. E. Cohen, W. E. Pickett, and H. Krakauer, *Phys. Rev. Lett.* **64**, 2575 (1990); J. R. Hardy and J. W. Flocken, *ibid.* **60**, 2191 (1988); N. M. Plakida, V. L. Aksenov, and S. L. Drechsler, *Europhys. Lett.* **4**, 1309 (1987).
- ⁴⁷S. K. Sinha, J. W. Lynn, T. E. Grierereit, Z. Hossain, L. C. Gupta, R. Nagarajan, and C. Godart, *Phys. Rev. B* **51**, 681 (1995).
- ⁴⁸D. W. Cooke, J. L. Smith, S. J. Blundell, K. H. Chow, P. A. Pattenden, F. L. Pratt, S. F. J. Cox, S. R. Brown, A. Morrobel-Sosa, R. L. Lichti, L. C. Gupta, R. Nagarajan, Z. Hossain, C. Mazumdar, and C. Godart, *Phys. Rev. B* **52**, R3864 (1995).
- ⁴⁹H. J. Trodahl, *Phys. Rev. B* **51**, 6175 (1995).